

Article

Not peer-reviewed version

Bone Regeneration with Stem Cells from Dental Pulp in a Rat Experimental Model

Haifa Hamad-Alrashid , Sandra Muntión , Fermín Sánchez-Guijo , [Javier Borrajo-Sánchez](#) , [Felipe Parreño-Manchado](#) , [M. Begoña García-Cenador](#) * , [F. Javier García-Criado](#)

Posted Date: 18 March 2024

doi: 10.20944/preprints202403.1012.v1

Keywords: DPSC; biomaterials; bone defect; osteogenesis; bone regeneration; angiogenesis; bioengineering; dental pulp; stem cells; bone graft



Preprints.org is a free multidiscipline platform providing preprint service that is dedicated to making early versions of research outputs permanently available and citable. Preprints posted at Preprints.org appear in Web of Science, Crossref, Google Scholar, Scilit, Europe PMC.

Copyright: This is an open access article distributed under the Creative Commons Attribution License which permits unrestricted use, distribution, and reproduction in any medium, provided the original work is properly cited.

Article

Bone Regeneration with Stem Cells from Dental Pulp in a Rat Experimental Model

Haifa Hamad-Alrashid ¹, Sandra Muntión ^{2,3}, Fermín Sánchez-Guijo ^{3,4,5}, Javier Borrajo-Sánchez ⁶, Felipe Parreño-Manchado ^{4,7}, M. Begoña García-Cenador ^{2,7,*} and F. Javier García-Criado ^{2,7}

¹ Doctoral School "Studii Salamantini", University of Salamanca, Salamanca, Spain; hrashed94@hotmail.com

² Biomedical Research Institute (IBSAL), Salamanca, Spain; smuntion@usal.es; mbgc@usal.es; fjgc@usal.es

³ Regenerative Medicine and Cellular Therapy Network Center of Castilla y León, Salamanca, Spain; ferminsg@usal.es; smuntion@usal.es

⁴ University Hospital of Salamanca, Salamanca, Spain; fparreno@usal.es; ferminsg@usal.es

⁵ Department of Medicine, Faculty of Medicine, University of Salamanca. Salamanca, Spain; ferminsg@usal.es

⁶ Department of Biomedical and Diagnostic Sciences, Faculty of Medicine, University of Salamanca. Salamanca, Spain; borrajo@usal.es

⁷ Department of Surgery, Faculty of Medicine, University of Salamanca, Salamanca, Spain; mbgc@usal.es; fjgc@usal.es; fparreno@usal.es

* Correspondence: mbgc@usal.es; Tel.: +34 663047442

Abstract: The increase in the rate and prevalence of diseases associated with the localized and general loss of bone mass calls for an investigation into therapeutic alternatives that largely involve the development of new biomaterials and cell therapy, converting tissue bioengineering into a promising option. An experimental model of a critical mandibular lesion in rats has been used to study bone regeneration by treating the osteotomy with the biomaterials Evolution[®] and Gen-Os[®] (OsteoBioI[®], Italy) combined, or not, with dental pulp stem cells (DP-MSC). The results obtained through the Micro-CT and histological study reveal the almost complete re-recovery of the lesion in the group with DP-MSC. These results are supported by increases in endoglin, TGF- β , protocollagen I, parathormone, and calcitonin, generating an environment of bone generation and development when combining Evolution[®] and Gen-Os[®] (OsteoBioI[®], Italy) with DP-MSC. These promising results confirm the transcendental role of DP-MSC in combination with osteogenic biomaterials for bone regeneration, and warrant further studies, including its assessment in clinical trials.

Keywords: DPSC; biomaterials; bone defect; osteogenesis; bone regeneration; angiogenesis; bioengineering; dental pulp; stem cells; bone graft

1. Introduction

The developed world has seen a sharp increase in the rate and prevalence of diseases associated with the localized and general loss of bone mass. Numerous studies have reported that many entities and medications are associated with this loss [1–6], which together with an increasingly sedentary lifestyle have a profound impact on bone metabolism [7]. Serious bone lesions are difficult to redress through autologous processes, which means that therapeutic procedures need to be used instead, but these are still limited [8].

Tissue engineering and cell therapies provide alternatives for inducing and promoting bone regeneration, focusing on personalized and precision regenerative medicine. Among other aspects, this reduces the morbidity of other treatments, such as surgery. The availability of biomaterials with an appropriate physical structure, adhesion potential, and cell proliferation, plays an influential role in the regeneration and repair of bone tissue [9–11], with a crucial factor being the advanced state of knowledge on stem cells [12–14] and on the growth factors that favor the differentiation and acceleration of these processes [15,16].

Given the scarce bioavailability of autologous grafts, the low osteoinductive capacity of xenografts appears to be the ideal solution. Cells, scaffolds (three-dimensional matrices or supports), and growth factors are the key factors [17], besides an appropriate physical-chemical environment. This requires the introduction of standardized protocols, from the gathering of cell material through to the establishment of clinical criteria, and this is the path taken by numerous studies.

This study assesses an experimental model of bone regeneration involving a mandibular defect in rats, using mesenchymal stem cells (MSCs) obtained from pulp material for finding a suitable biological substitute for regenerating critical bone defects and increasing the potential of MSCs through biological supports with a high concentration of osteogenic factors.

2. Results

2.1. Obtaining Dental Pulp Mesenchymal Stem Cells (DP-MSC)

The DP-MSC were successfully obtained from the molar pulp chamber (Image 1).

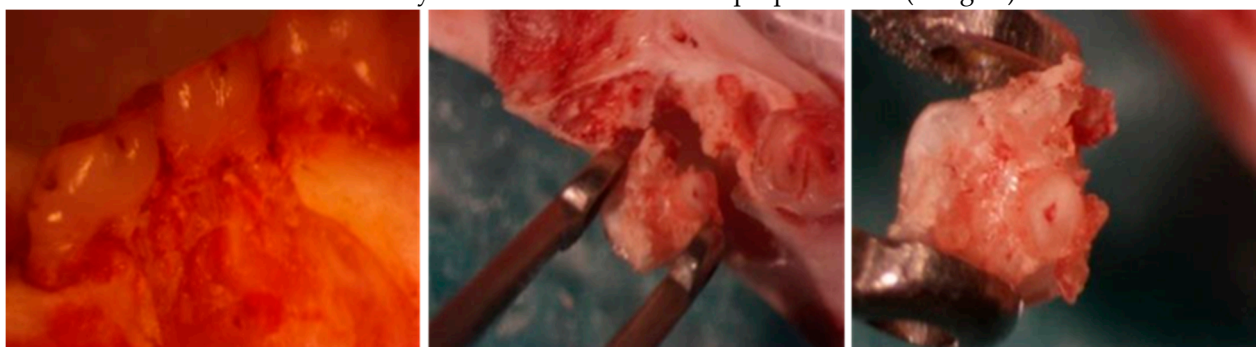


Image 1. Extraction of pulp.

2.2. Cell Culture and Expansion

The results show that MSCs can be isolated by applying enzymatic digestion methods to dental pulp tissue. The cells obtained from the culture had a long and flat fibroblast-type morphology and were attached to the plastic surface on the culture, as essential characteristics of MSCs (Image 2).

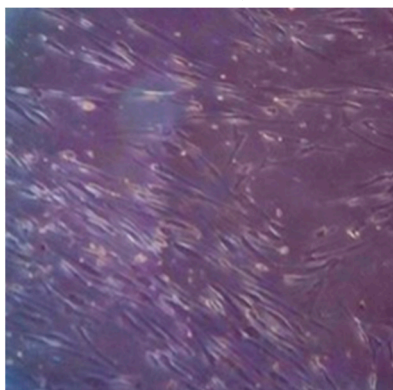


Image 2. Confluence of MSCs under optical microscopy.

2.3. Characterisation. Flow Cytometry

The cultures from each specimen were investigated for the percentage of MSCs by flow cytometry, using the following panel: CD49e PE (HMa5-1, BioLegend® cat. 103905), 7-AAD (BioLegend® cat. 420403), CD11b/c PE-Cy7 (OX-42, BioLegend® cat. 201817), CD29 APC (HMb1-1, Miltenyi Biotec cat. 130-123-829), CD90-1 APC-/Fire™ 750 (Thy1.1, BioLegend® cat. 202543), and CD45 Pacific Blue™ (OX-1, BioLegend® cat. 202225). The samples were acquired in the BD FACSCanto™ II System and the data were analysed using FlowJo™ Software (v. 10, ©Becton Dickinson & Company).

The gating strategy used for analyzing the MSC population is illustrated in Figure 1. The percentage of MSCs was calculated from live cells that did not express lineage markers (CD45 and CD11b/c) and which expressed CD90 and CD29 simultaneously.

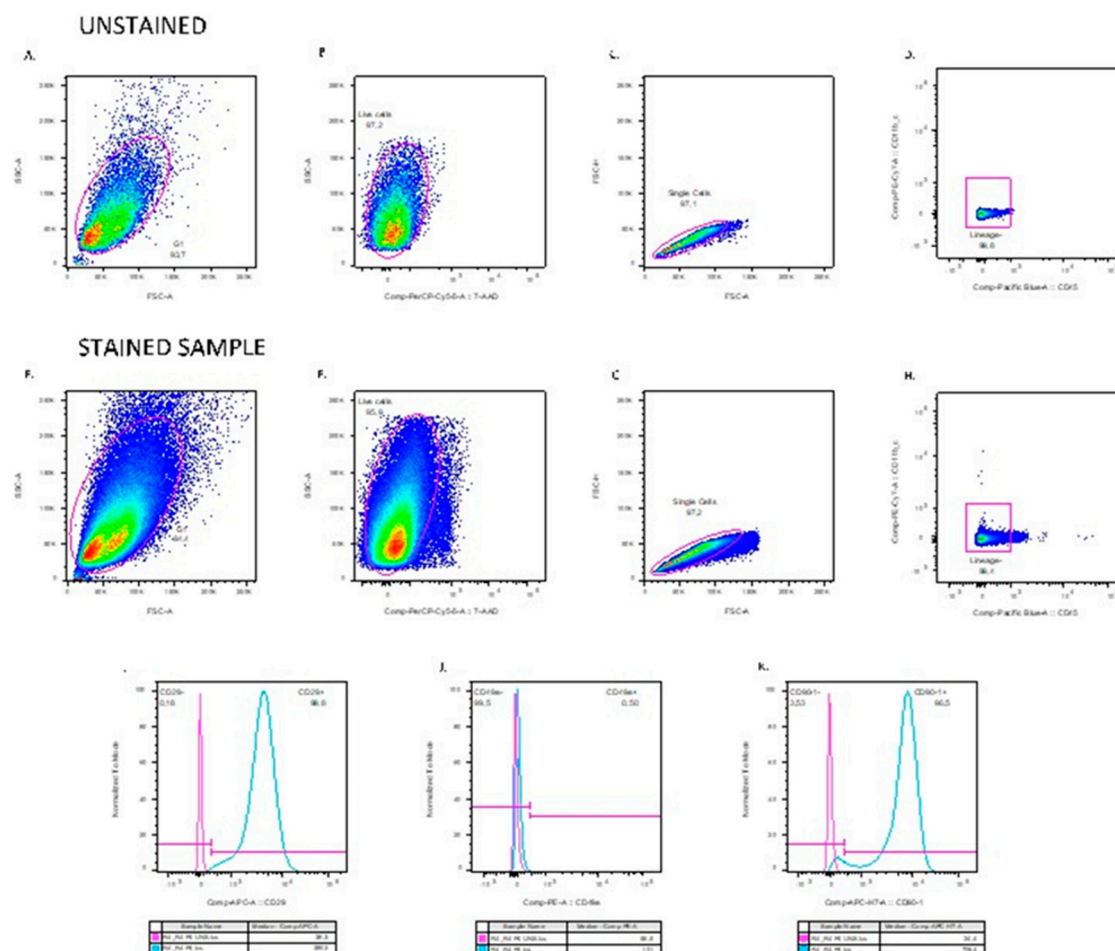


Figure 1. Illustration of the gating strategy used to identify the MSC population in the rat dental pulp isolates. The gates were determined in the unstained sample (A-D) and applied to the stained sample (E-H). The size and complexity gate (A, E), and the live cells were selected (B, F), followed by the doublet exclusion (C, G). The lineage negative population was then gated (D, H), and the expression of CD29, CD49e, and CD90-1 was analysed as shown in histograms I, J, and K.

In total, from six rats, this population of MSCs was identified in $94.58\% \pm 3.62$ of the isolates. From step two all the samples already presented 90% of the population with the characteristics of the MSCs (Lineage-CD90-1+CD29+) and were maintained until step 10.

2.4. Verifying the Cell Viability of the Implants

Following the surgery, the remains of the vials were seeded on plates. Within a few days' cells appeared attached to the plate, and were therefore viable and proliferating.

2.5. In Vivo Results in the Experimental Model

An essential step in our assay involved creating a critical bone defect on the mandible that was large enough to avoid spontaneous regeneration. A critical defect is defined as one that regenerates less than 10% of the bone during the animal's lifetime [18], and in a rat mandible this will mean an area of more than 4 mm in diameter [19–21].

None of the specimens died in the post-operative period, nor recorded fractures, with a mandibular defect of 5 mm in diameter in all cases.

The overall condition of the specimens was good in all the groups, with some swelling of soft tissue due to the osteotomy, which disappeared spontaneously.

The post-surgical clinical monitoring of the specimens treated did not reveal any rejections or degenerative changes due to the dental lesion. The membrane recorded bioresorption, low immunogenicity, stability, and prolonged protection of the covered graft.

2.5.1. CONTROL Group

Study with microcomputed tomography (microCT)

Image 3 shows the defect on the mandible in the Control group, prior to its resection at three (A) and six (B) months of the study.

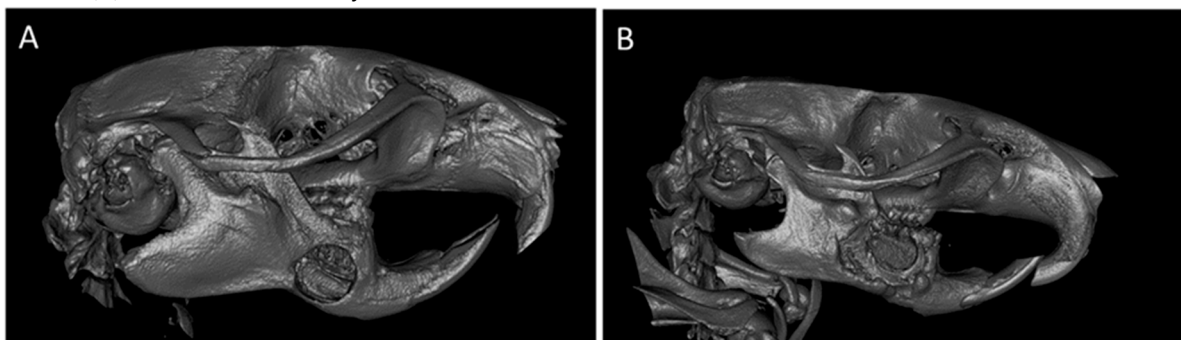


Image 3. MicroCT image of a defect in Group C at 3 (A) and 6 months (B).

2.5.2. G+M Group

Study with microcomputed tomography (microCT)

At three months, we observed a significant collapse of the soft tissues and a minor restitution of the defect. The biomaterial has not diminished in volume. The radiopacity of the lesion is highly heterogenous in the center of the defect (Image 4 C).

At six months (Image 4 D), a highlight is the geometric morphology of the defect, which has become smaller, acquiring a denser appearance and with significant irregularity in its perimeter and a significantly greater radiological density than in the preceding state and greater uniformity, although the granulated aspect remained. There is an attempted formation of trabeculae between the biomaterial and the cortical, with the hazy appearance of dense bone pathways in the defect treated with the membrane + scaffold, compared to the situation at three months (Image 4 C).

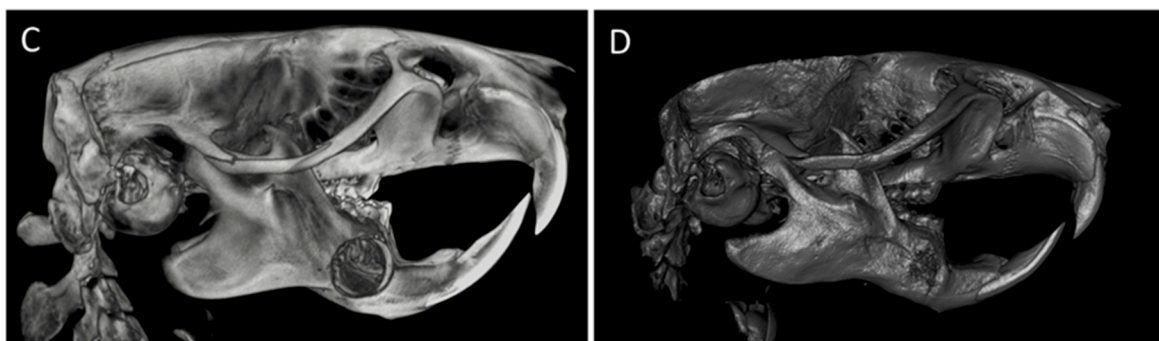


Image 4. MicroCT image of a defect in the G+M Group at 3 months (C). CT image of a defect in the G+M Group at 6 months (D).

2.5.3. G+M+S Group

Study with microcomputed tomography (microCT)

At three months, uniform levels of radiopacity were recorded, with significant consistency in the perimeter and partial structural restoration with new bone (Image 5 E). At six months, there was

almost complete radiological repair of the defects in all cases (80-100%), revealing a high consistency with the bone perimeters and a very uniform distribution of the radiological density (Image 5 F).

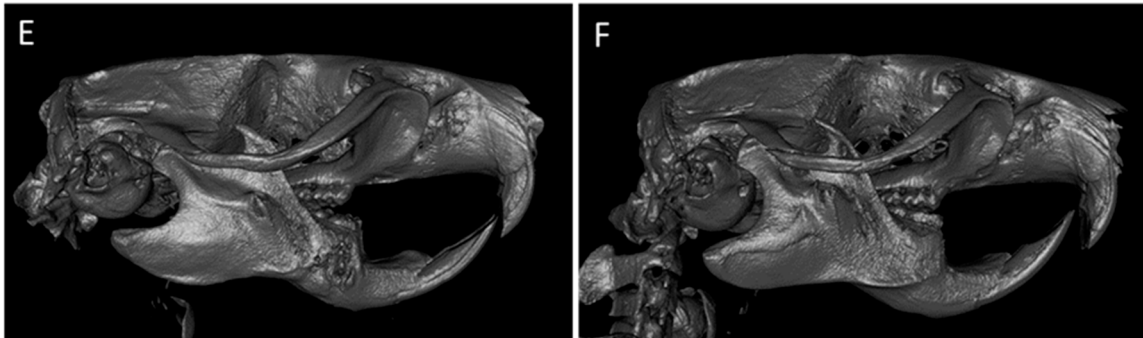


Image 5. MicroCT image of a defect in the G+M+S group at 3 months (E). Radiological image of a defect in the G+M+S group at 6 months (F).

2.6. Descriptive Histological Analysis

The untreated Control group recorded a fibrous cicatricial reaction, sometimes overrunning the edges of the wound, with no signs of bone regeneration in either of the two timeframes studied (Image 6).

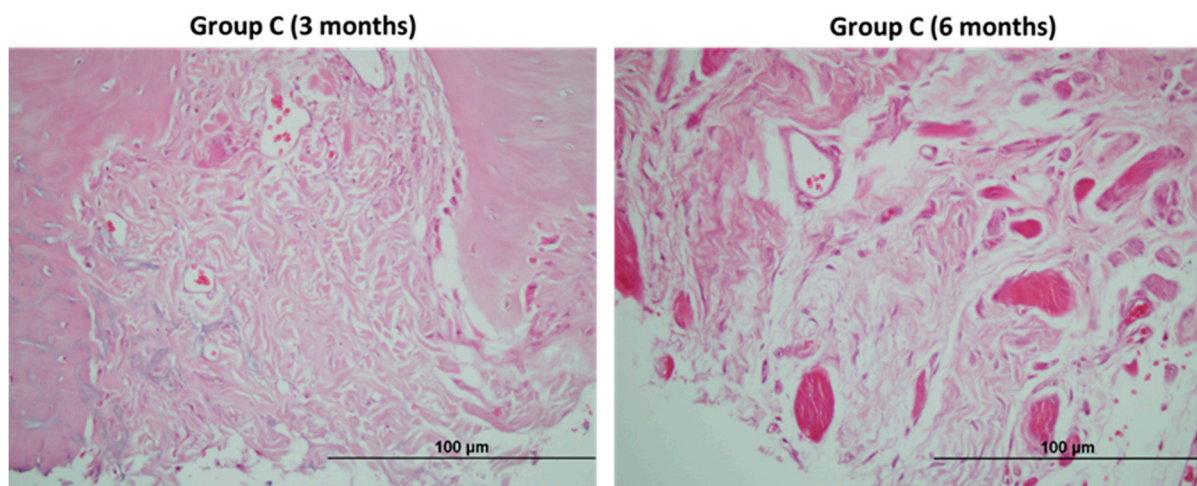


Image 6. Fibrous reaction of an untreated lesion. The fibrous cicatricial reaction overran the edges of the lesion. There is no sign of any reactive bone regeneration.

At three months, one of the treated groups, G+M (A), showed few signs of bone regeneration, and the edges of the lesion were readily observable. Particles of biomaterial could be seen together with chronic inflammatory infiltration with the presence of multinucleated giant cells (Image 7).

For the same timeframe, the other treated group G+M+S (B) revealed major cellularity, with a considerable decrease in inflammatory reaction bone-forming activity. It recorded osteoclastogenesis and neoformed bone trabeculae surrounding the biomaterial. There are active osteoblasts and, in some cases, neoformed bone trabeculae around the biomaterial. There are areas with osteoblast precursor cells and osteoblasts partially included in the osteoid, which they are calcifying. There is also abundant immature reticular bone together with osteocytes in the lines of bone development (Image 7).

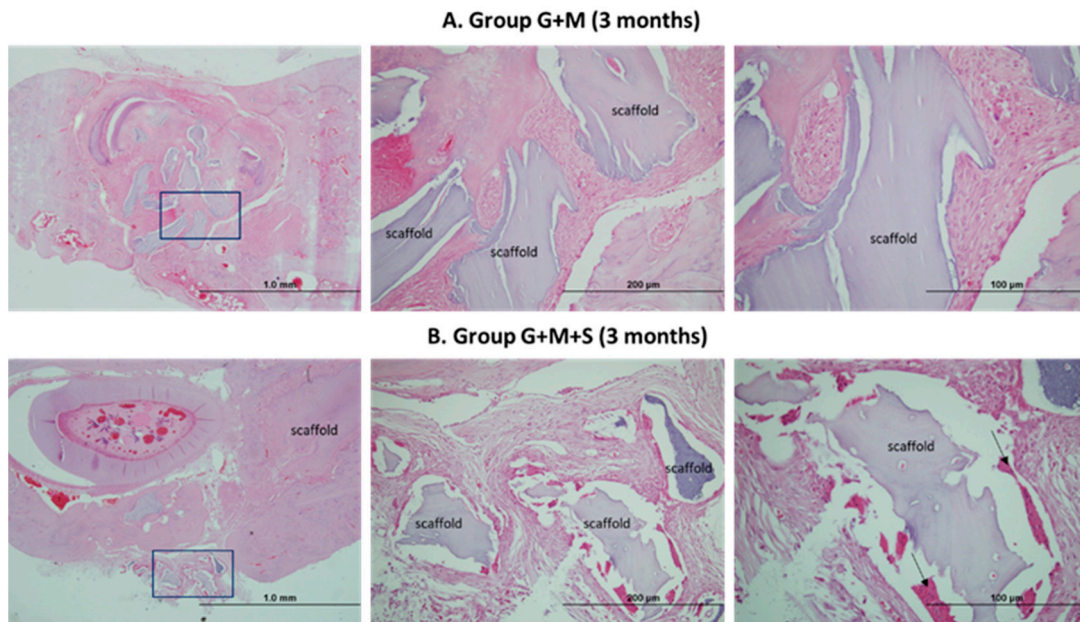


Image 7. Haematoxylin/eosin of the bone defect at three months. G+M group. Various particles of biomaterial and chronic inflammatory component (A). G+M+S group. Osteogenesis. Black arrows: osteoblasts included in the osteoid (B).

At six months, the treated G+M group continued to have particles of biomaterial encapsulated in a fibrotic matrix. The only signs of new bone were on the edges of the lesion, with a chronic inflammatory component. By contrast, the group treated with DP-MSC records full bone regeneration with well-organized, vascularized bone with a lamellar structure surrounded by haversian canals. The edges of the lesion are not distinguishable (Image 8).

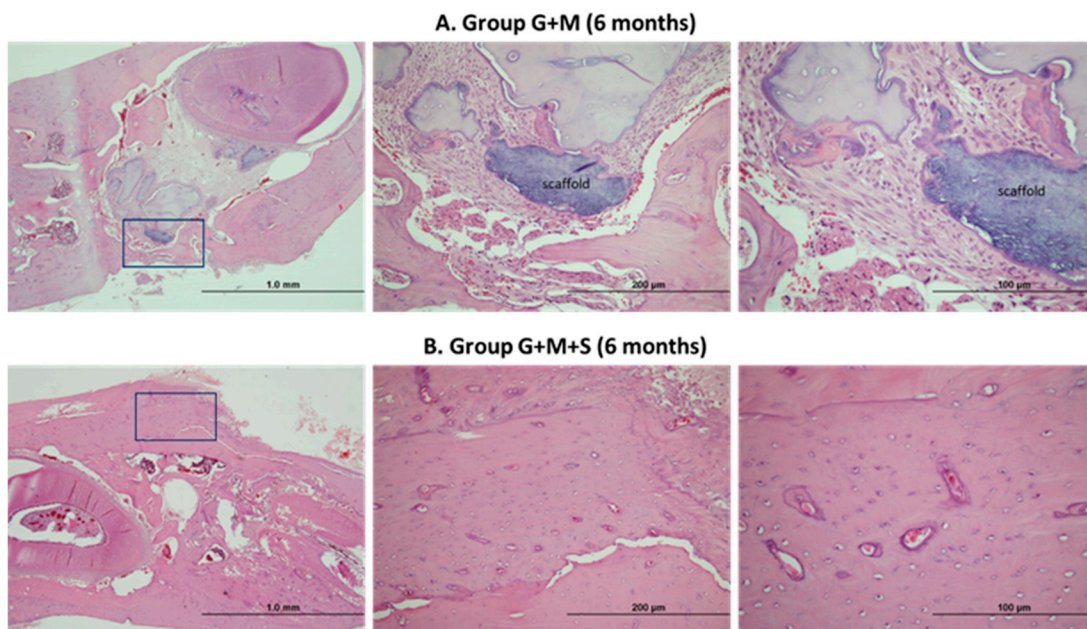


Image 8. Haematoxylin/eosin of the bone defect at six months. G+M group. Chronic inflammation (A). G+M+S group. Osteogenesis (B).

2.7. Molecular Studies

At three and six months, an assessment was made of the TGF- β growth factor and the levels of type 1 procollagen, the serum concentrations of the calciotropic hormone calcitonin and the parathyroid hormone (PTH), and the endoglin expression.

As the neovascularization marker, we studied the endoglin crucial for TGF- β signaling in the endothelial cells. The results for the G+M+S group at three months reveal a significant increase in both endoglin expression and the production of growth factors such as TGF β 1. No changes were found in either the serum levels of endoglin or TGF β 1 in any of the groups at six months (Figures 2 and 3).

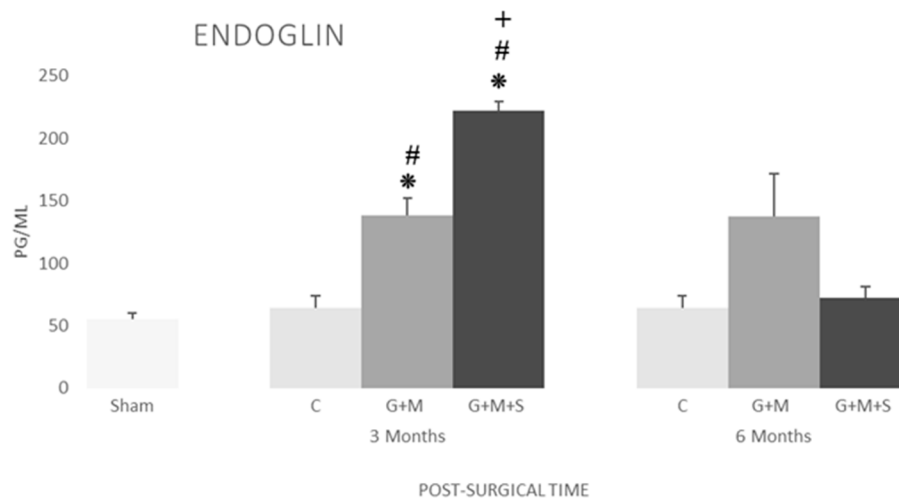


Figure 2. Serum concentration of endoglin (pg/mL) in the various groups at 3 and 6 months. * $p < 0.05$ compared to the Control group; # $p < 0.05$ compared to the Sham group; + $p < 0.05$ compared to the G+M group (Kruskal-Wallis multiple-comparison test and Dunn test).

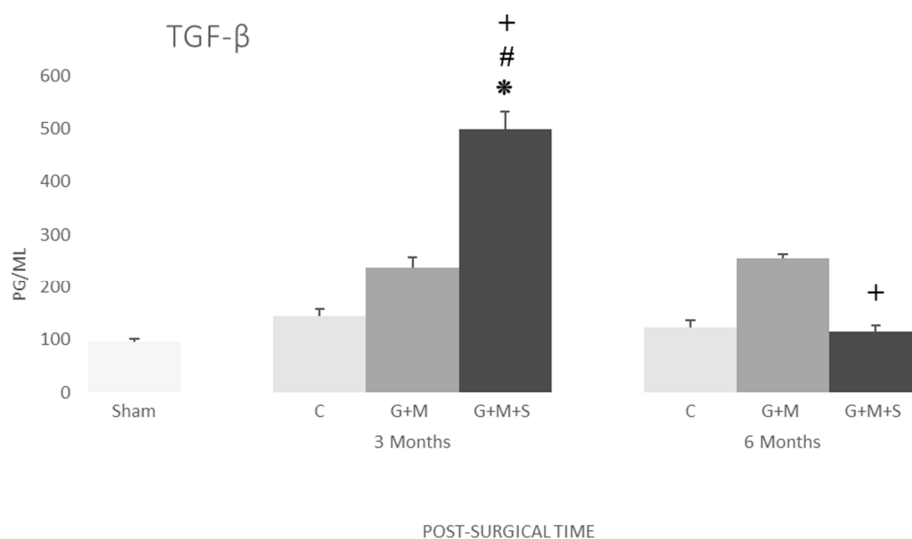


Figure 3. Serum concentration of TGF- β 1 (pg/mL) in the various groups at 3 and 6 months. * $p < 0.05$ compared to the Control group; # $p < 0.05$ compared to the Sham group; + $p < 0.05$ compared to the G+M group (Kruskal-Wallis multiple-comparison test and Dunn test).

The serum levels of procollagen I were higher in the treated groups at three months compared to the Sham and Control groups, with no differences between them. The G+M group at six months continued to record higher serum levels than the Sham and Control groups, while in the G+M+S groups these levels were similar to those in the Sham group (Figure 4).

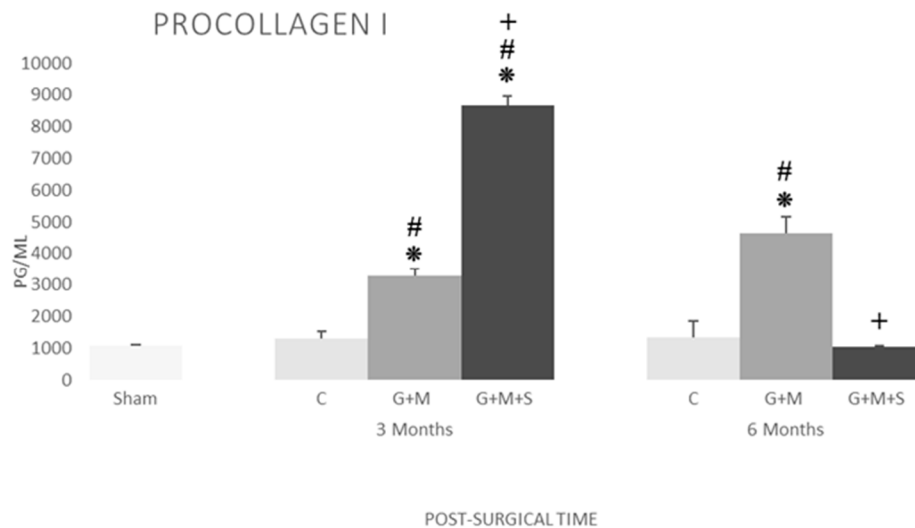


Figure 4. Serum concentration of procollagen (pg/mL) in the various groups at 3 and 6 months. * $p < 0.05$ compared to the Control group; # $p < 0.05$ compared to the Sham group; + $p < 0.05$ compared to the G+M group. (Kruskal-Wallis multiple-comparison test and Dunn test).

Following the lesion, we observed higher levels of PTH in all the groups compared to the Sham group, except for the Control group at three months and the G+M+S group at six months. At the same time, the treated groups maintained high serum levels compared to the Control group, with the exception of the G+M+S group at six months (Figure 5).

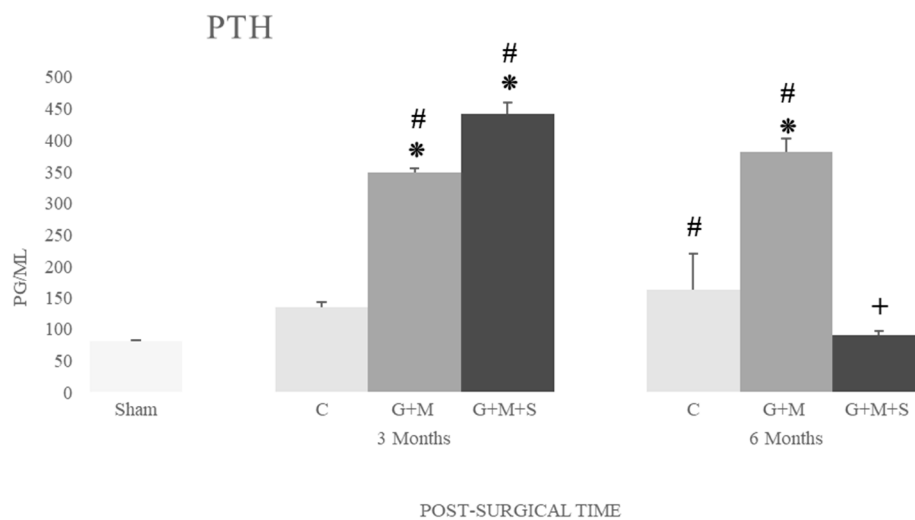


Figure 5. Serum concentration of parathormone (pg/mL) in the various groups at 3 and 6 months. * $p < 0.05$ compared to the Control group; # $p < 0.05$ compared to the Sham group; + $p < 0.05$ compared to the G+M group (Kruskal-Wallis multiple-comparison test and Dunn test).

No changes were found in the serum levels of calcitonin in the Sham, Control, and G+M groups. The G+M+S group, however, recorded a significant decrease at three months, attaining the Sham group's levels after six months (Figure 6).

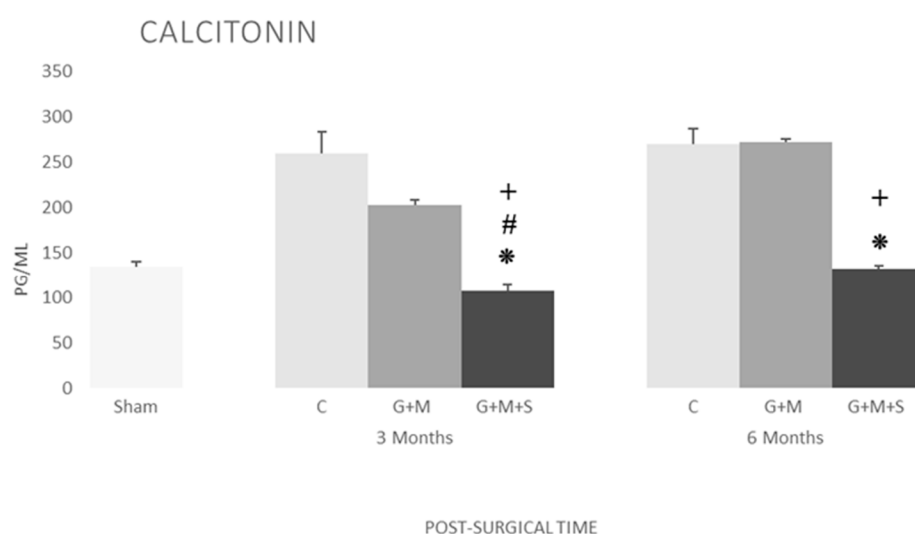


Figure 6. Serum concentration of calcitonin (pg/mL) in the various groups at 3 and 6 months. * $p < 0.05$ compared to the Control group; # $p < 0.05$ compared to the Sham group; + $p < 0.05$ compared to the G+M group (Kruskal-Wallis multiple-comparison test and Dunn test).

3. Discussion

Our study confirms once more the accessibility of dental pulp to efficiently extract DP-MSC. The experimental model used is ideal for studying the efficacy of DP-MSC in osteogenesis, adjudging it to be financially viable with a high performance.

Although the characterization for human derived-MSCs has a well-established criterion, rat MSCs still lack the same consistency, mostly regarding surface markers. Some markers, such as CD29 and CD90 were more frequent, while others (e.g., CD73, CD105, CD44, and CD49e) were less so [22–27]. Isolates were evaluated here for the presence of the CD29, CD90 and CD49e expression and the absence of the expression of lineage markers, CD11b/c and CD45. The presence of the MSC population was confirmed in all the samples tested by the Lineage-CD29+CD90+ profile. Interestingly, the samples did not express the CD49e marker. Known as $\alpha 5$ integrins, this molecule associates non-covalently with CD29, a $\beta 1$ integrin, to form the fibronectin receptor [28]. The relatively low percentage of the CD49e+ population, ranging from 1-30%, might be explained by the sensitivity of the integrins $\alpha 5\beta 1$ to trypsin [29,30]. The use of this proteolytic enzyme could therefore alter the antibody binding site, diminishing its recognition by the clone of the antibody used. Nevertheless, at the same time, the expression of CD90 and CD29 and the absence of lineage markers identify the MSC population.

The results from the radiological and histological studies confirm that there is no evidence of osteogenic activity in either Group C or in the G+M group, confirming that these conditions require enough cell material and a high osteogenic capability. A major characteristic of DP-MSC that makes them a promising osteogenic candidate is their co-differentiation in osteoblasts and endotheliocytes, fully integrating the blood vessels within the ossification lines, prompting the formation of vascularized bone tissue [31,32]. A clinical trial conducted in 2019 [33] has found that these cells produce extracellular vesicles (EVs) that contain pro-angiogenic factors (e.g., VEGF, angiopoietin, or angiogenin). The Gen-Os® biomaterial's angiogenic potential is also greater than other synthetic materials, as it favors the secretion of VEGF [34].

DP-MSC are therefore the mainstay of the osteogenic process ending at six months, with full bone formation. DP-MSC contain immunomodulating and anti-inflammatory factors such as IL-6,

IL-8, transforming growth factor-beta (TGF- β), hepatocyte growth factor (HGF), and indoleamine 2,3-dioxygenase (IDO) [35,36], all of which play an important part in regulating the equilibrium between the anti- and pro-inflammatory properties of cytokines [36–39], suppressing the activation of T cells, the proliferation of peripheral blood mononuclear cells, and even allogeneic immune responses [35,38–40].

In this study, the endoglin in the group treated with DP-MSc at three months, and like TGF- β , recorded high levels of expression, with this protein being part of the receptor complex of TGF- β that is highly expressed in several kinds of proliferating cells and stem cells in differentiation during the initial stages of wound healing. Angiogenesis is a major step in bone healing, and endoglin is highly expressed in proliferating endothelial cells and pericytes during angiogenesis. This means it is not only a proliferation marker, as it also regulates cell functions such as adhesion, migration, and cell permeability. Endoglin has a significant role to play in the regulation of the movement of stem cells from a specific niche to the damaged region [41]. Besides high levels of TGF- β 1, our results have revealed an increase in collagen I content in the G+M+S group at three months, confirming that the TGF- β 1 factor is involved in cell differentiation and collagen synthesis [42]. As type I collagen is the main component of the organic matrix, this increase in our results will render the bone tissue flexible and resistant to impact loads [43].

TGF- β regulates the proliferation and differentiation of chondrocytes and osteoblasts [44,45], although mainly, its osteoinductive properties render it a major growth factor, performing a key role in the different stages of the bone healing process [46] by regulating the production of the extracellular matrix (ECM), proteases, protease inhibitors, migration, chemotaxis, and the proliferation of different kinds of cells, including stem cells, which regulate angiogenesis and the formation of granulation tissue, remodeling of the matrix, and scar maturation.

The implementation of DP-MSc on the biomaterials also increases the serum levels of PTH at three months, favoring bone regeneration, as it has osteoclastic and osteogenic activity, whereby the bone formation process promoted by the PTH is very similar to the same process in physiological conditions. Bone repair is not a unique osteogenic process and requires angiogenesis and the participation of osteoclasts [47]. Bone repair without osteoclastic activity may lead to excessive bone development [48]. PTH has been shown to regulate the differentiation pathway of bone marrow mesenchymal stem/stromal cells (BMSC), increase their osteogenic differentiation, and inhibit their adipogenic differentiation [49–53].

The study has also found a reduction in the serum concentration of CT in the group treated with DP-MSc. The changes observed in the levels of calciotropic hormones in rats could increase bone resorption and promote mineral metabolism in the DPSC group [54,55].

The alloplastic matrices take a backseat as the mere facilitator of cell functions, although it is essential to use the most appropriate ones to provide cell support and facilitate regeneration with osteoinductive factors. Each bone substitute has different properties, and Gen-Os® (OsteoBiol®, Italy) appears to provide the best guarantees for osteogenesis. Indeed, an assay [56] shows that the proliferation and recruitment of MSC is higher with Gen-Os® (OsteoBiol®, Italy) than with other alloplast grafts such as Bio-Oss®. It also produces a smaller inflammatory reaction than other synthetic biomaterials [57].

It seems fair to say that the properties of the different elements used together favour osteogenesis, acting as an ideal bone substitute and enabling the bone to regenerate while upholding all its characteristics.

4. Materials and Methods

The sample consisted of 46 Wistar Han™ (RccHan™:WIST) adult male rats (8 months - 350 g) supplied by Harlan Laboratories Models, S.L.

All the experiments were conducted following the guidelines established by Spain's Royal Decree 53/013 (Approval by the Ethics Committee at Salamanca University, filed under number 361).

4.1. Experimental Design, Specimens, and Groups (Figure 7)

The molars of rats were used for the extraction of DP-MSC (two pulps per extraction), as described in due course (N = 6).

The 40 remaining rats were distributed into the following groups:

- Sham (Sham): Subject to the same anesthetic/surgical technique as the other groups except for the bone lesion and its treatment, as indicated below. The specimens remained caged for three months, whereupon the samples were gathered and they were euthanized (N = 4).
- Control (C): The bone lesion was effected but not treated, as indicated below. The specimens remained caged for three and six months (N = 6 in each case), whereupon the samples were gathered and they were euthanized (N = 12).
- Gen-Os® + Evolution® (G+M): The bone lesion was effected and then treated with the substitute bone biomaterial and covered with resorbable membrane, as indicated below. The specimens remained caged for three and six months (N = 6 in each case), whereupon the samples were gathered and they were euthanized (N = 12).
- Gen-Os® + Evolution® + DPSC (G+M+S): The bone lesion was effected and then treated with the substitute bone biomaterial plus DP-MSC and covered with resorbable membrane, as indicated below. The specimens remained caged for three and six months (N = 6 in each case), whereupon the samples were gathered and they were euthanized (N = 12).

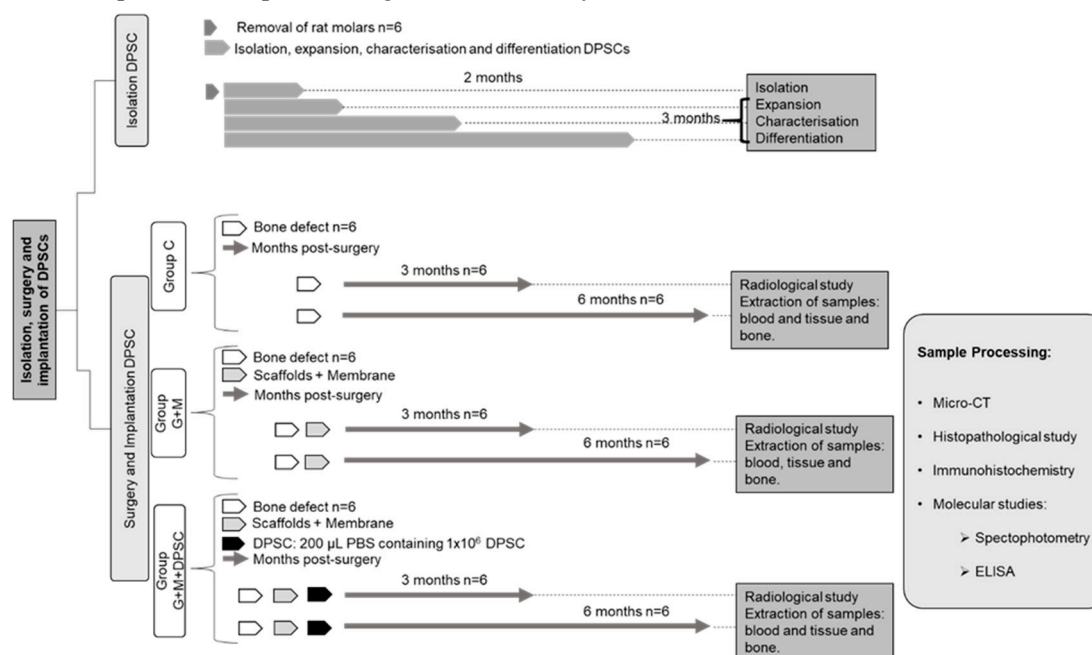


Figure 7. Flowchart scheme of the study's experimental design.

4.2. Biomaterials

The Evolution® (OsteoBiol®, Italy) resorbable membrane used involved dense collagen fibres that covered the induced bone defect.

The Gen-Os® (OsteoBiol®, Italy) 250-1000 µm granulated bone substitute used was of biological origin (pig) based on hydroxyapatite (HA) and type I collagen. Its composition is 80% spongy bone and 20% cortical with high osteoconductivity. This three-dimensional matrix provided the support for the MSCs from the dental pulp.

4.3. Obtaining the DP-MSC from Pulp Tissue

Rat molars were extracted under general intraperitoneal anesthetic, and the specimens were then euthanized with an anesthetic overdose.

The molars were then crushed with a gouge forceps, obtaining pulp tissue with a Hemingway® bone curette (Model 1145/0).

The samples were placed in a falcon tube (50 ml) with 30 ml of DMEM (Dulbecco's Modified Eagle Medium®, Invitrogen), supplemented with penicillin (100 U/ml), streptomycin (100 µg/ml), and fetal bovine serum (FBS) at 10% (Invitrogen), and cold stored for a maximum of six hours.

For enzymatic disaggregation, the tissue was incubated for 70 minutes at 37°C and shaken with collagenase I (at 0.2%) (Worthington Biochemicals Corporation®) and dispase II (at 0.4%) (Sanko Junyaku Co. Ltd, Tokyo, Japan). It was centrifuged for 10 minutes at 1200 rpm, and the sediment was spread on 9 cm² plates and incubated at 37°C.

Cell culture and growth was performed by incubating the cells at 37°C in a humid environment with 5% CO₂ in a DMEM (Dulbecco's Modified Eagle Medium®), supplemented with FBS (10%) (Equitech-Bio Inc., Kerrville, TX) and with penicillin (100 U/ml) and streptomycin (100 µg/ml). The culture medium was replaced twice per week, and any unattached cells were discarded.

The culture was maintained until a cell confluence of at least 80-90% was reached, whereupon the culture medium was eliminated, washed with sterile phosphate buffered saline - PBS (Invitrogen Corporation, Paisely, UK®) and incubated for five minutes at 37°C with trypsin 1 (0.05%) (Invitrogen Corporation, Paisely, UK®).

Trypsin 1 was neutralized before the addition of a culture medium for MSCs. Cellularity was increased by again seeding a concentration of 5,000 cells/cm² in larger beakers, up to step 10 (S10).

Cells were isolated for their immunophenotypic characterisation and induction to differentiation in several steps (1, 3, 6, and 10) to verify their osteoblastic capacity. Two parallel samples were cultivated under the same conditions (at 37°C, 5% CO₂, and > 90% humidity): one for osteoblast differentiation and the other as control.

The medium for osteogenic differentiation (NH OsteoDiff Medium, Miltenyi Biotec, Germany) contained β-glycerol-phosphate, ascorbic acid-2-phosphate, dexamethasone, and FBS. The cultures were maintained for 10 days and the medium was changed every 3-4 days. They were then washed with PBS cold 70% ethanol fraction (Merck KGaA, Darmstadt, Germany) and fixed for 10 minutes.

Osteoblast differentiation was confirmed by observing alkaline phosphatase activity by staining for 20-30 minutes with NBT/BCIP (Nitroblue tetrazolium chloride 5-bromo-4-chloro-3-indolyl-phosphate, Roche, Basel, Switzerland), and contrasting for two minutes with hematoxylin (1 mL) (Merck KGaA, Darmstadt, Germany).

4.4. Surgical Procedure

All the surgical procedures were performed under strictly sterile conditions in a laminar flow cabinet.

Following intraperitoneal anesthetization with a mixture of xylazine, ketamine, and saline solution (ratio 2:3:3, at a dose of 0.2 mL/100 g body weight), the surgical area was shaved and an antiseptic solution of povidone-iodine (Betadine, Asta Medica®) was applied.

A 15 mm longitudinal incision was made 2 mm above the lower edge of the mandibular body, providing submandibular entry, accessing the ascendant branch and angle of the right jaw, where a 5 mm diameter circular bone lesion was made with an electric micromotor and 5 mm trephine drill, and considered to be a critical bone defect (Image 9). The bone defect was subsequently covered as described for each group and the incisions were closed in layers. The specimens were caged in a state of good health until three or six months had elapsed after surgery, with direct ad libitum access to food and water.



Image 9. Access to the insertion crest. Circular osteotomy with trephine drill.

The post-surgical clinical monitoring involved assessing the specimens' overall condition, the appearance of the wound and surgical area, bleeding or discharge from the wound, rejection of the biomaterials, and any degenerative changes due to the dental lesion.

Once the monitoring period had ended, the next step involved gathering the samples and euthanising the specimens:

- Total blood by aortic puncture, centrifuged (20 minutes at 4500 rpm and 4°C), extraction of plasma, aliquoted, and frozen at -80°C.
- Perilesional tissue (bone and muscle) placed in liquid nitrogen and stored at -80°C.
- Affected mandibulae removed in bloc, removal of the tissue on the bone surface, with some being immersed in formaldehyde 3.7-4.0% w/v buffered to pH = 7, and others stored at -80°C.

4.5. Verification of Cell Viability

The DP-MSD inserted in the biomaterial were viable, with a small volume of the implanted cells being retained and returned to the laboratory for re-seeding.

4.6. Macroscopic Study

Prior to euthanizing, a descriptive assessment was made of the following: anatomic and tissue formation; signs of infection; existence of fractures; presence or disappearance of biomaterials; degenerative dental transformations; bone sequestrations; surface morphology, and solidity of the defect.

4.7. Scanning with Micro-Computed Tomography (micro-CT)

Once the period of monitoring had elapsed, and prior to euthanizing, two specimens for each period of evolution and group were subject to an x-ray evaluation through micro-computed tomography (mCT) with SuperArgus equipment from SEDECAL Medical Systems.

The evaluation addressed the regeneration of the defect in the four groups and the different timeframes, together with the changes in the morphology of the biomaterial following its implanting.

It also considered the biomaterial's loss of homogeneity over the study period as a process of integration in the host bone and remodeling.

Bone trabeculae were also detected within the biomaterial.

The biomaterial's dispersion within the medullary cavity was studied, together with the appearance on the periphery of the implanted area of bone trabeculae forming "bridges" between the biomaterial and the adjacent bone cortical.

4.8. Histomorphometric Evaluation

The hemimandibles were obtained and fixed in 4% formalin for 48 hours before being immersed in 10% EDTA for 30 days. The bone tissues were then embedded and the paraffin blocks were cut

into 4 μm sections. The sections from each sample were stained with hematoxylin-eosin (H&E) for their comparative histological study with optical microscopy (Olympus, Tokyo, Japan).

4.9. ELISA

This technique was used to determine the concentrations of calcitropic hormones such as calcitonin (CT) and parathormone (PTH), the growth factor TGF- β , the levels of type I procollagen, and the endoglin expression, in the serum of the rats in each group. This involved commercial kits, and the procedures followed the manufacturer's instructions. Parathyroid Hormone (PTH): Enzyme-linked Immunosorbent Assay kit ABK1-E1599. Calcitonin: Enzyme-linked Immunosorbent Assay kit ABK1-E1354. Collagen Type 1 Alpha 2(COL1 α 2): Enzyme-linked Immunosorbent Assay kit ABK1-744. Transforming Growth Factor Beta 1 (TGF β 1): Enzyme-linked Immunosorbent Assay kit ABK1-E1239. Endoglin (ENG): Enzyme-linked Immunosorbent Assay kit ABK1-E2467.

4.10. Statistical Study

The quantitative data have been represented as $X \pm \text{SD}$ (mean \pm standard deviation). A value of $p < 0.05$ was accepted as a significant result. The statistical software used was NCSS 2007 and Gess 2006 - Version: 07.1.21 - Released 1 June 2011 (Dr Jerry L. Hintze, Kaysville, Utah, USA).

5. Conclusions

Our experimental study shows that the combination of DP-MSC with Gen-Os[®] (OsteoBiol[®], Italy), as bone substitute, and the Evolution[®] (OsteoBiol[®], Italy) membrane successfully regenerates the bone in critical mandibular defects in rats, without any apparent complications. This conclusion is based on the major osteogenic and angiogenic capacity of DP-MSC, as a promising tool because of their great potential for the regeneration or engineering of dental and oral tissues. The cell therapy associated with the high concentration of osteoinductive factors in the biomaterial could become the ideal combination in the treatment of bone defects. Nevertheless, further research is required on action mechanisms, therapeutic dosages, and other possible variables that may alter the results. The control of bone regeneration requires a thorough understanding at cellular and molecular level. Understanding how and when signaling molecules control angiogenesis, migration, proliferation, and the differentiation of dental stem cells will open new horizons for all the procedures involving bone regeneration. Although the data gathered thus far are promising, we need to continue exploring this field with a view to its clinical application.

Author Contributions: Conceptualization, F.J.G.C., H.H.A., and M.B.G.C.; methodology, F.J.G.C., H.H.A., J.B.S., and M.B.G.C.; validation, F.J.G.C., H.H.A., and M.B.G.C.; formal analysis, F.J.G.C.; investigation, H.H.A., M.B.G.C., F.P.M. and S.M.O.; resources, J.B.S., M.B.G.C. and S.M.O.; writing—original draft preparation, F.J.G.C., F.S.G., S.M.O., and M.B.G.C.; writing—review and editing, F.J.G.C., F.S.G., S.M.O., and M.B.G.C.; visualization, H.H.A. S.M.O., and M.B.G.C.; supervision, F.J.G.C., and F.S.G.; project administration, F.J.G.C., and MBGC; funding acquisition, F.J.G.C., and H.H.A. All authors have read and agreed to the published version of the manuscript.

Funding: This research was funded by Haifa Al-Rashed Dental Clinic, located at 8078 King Abdul Aziz Rd, Ar Rabi, Riyadh 13315 (Kingdom of Saudi Arabia).

Institutional Review Board Statement: The animal study protocol was approved by the Ethics Committee at Salamanca University, filed under number 361.

Informed Consent Statement: Not applicable.

Data Availability Statement: Data that do not appear in the article are available from the authors upon request.

Acknowledgments: We thank Daniel López Montañés, technical support of Biosanitary Research Institute (IBSAL), for their great help in the transport and maintenance of the animals.

Conflicts of Interest: The authors declare no conflicts of interest.

References

1. Diana, A.; Carlino, F.; Giunta, E.F.; Franzese, E.; Guerrera, L.P.; Di Lauro, V.; Ciardiello, F.; Daniele, B.; Oritura, M. Cancer Treatment-Induced Bone Loss (CTIBL): State of the Art and Proper Management in Breast Cancer Patients on Endocrine Therapy. *Curr Treat Options Oncol* **2021**, *22*, 45, doi:10.1007/s11864-021-00835-2.
2. Stumpf, U.; Kostev, K.; Kyvernitakis, J.; Böcker, W.; Hadji, P. Incidence of fractures in young women with breast cancer - a retrospective cohort study. *J Bone Oncol* **2019**, *18*, 100254, doi:10.1016/j.jbo.2019.100254.
3. Vestergaard, P. Drugs Causing Bone Loss. *Handb Exp Pharmacol* **2020**, *262*, 475-497, doi:10.1007/164_2019_340.
4. Osipov, B.; Emami, A.J.; Christiansen, B.A. Systemic Bone Loss After Fracture. *Clin Rev Bone Miner Metab* **2018**, *16*, 116-130, doi:10.1007/s12018-018-9253-0.
5. Pluskiewicz, W.; Adamczyk, P.; Drozdowska, B. Fracture risk and fracture prevalence in women from outpatient osteoporosis clinic and subjects from population-based sample: A comparison between GO Study and RAC-OST-POL cohorts. *Adv Clin Exp Med* **2022**, doi:10.17219/acem/152736.
6. Ruchlemer, R.; Amit-Kohn, M.; Tvito, A.; Sindelovsky, I.; Zimran, A.; Raveh-Brawer, D. Bone loss and hematological malignancies in adults: a pilot study. *Support Care Cancer* **2018**, *26*, 3013-3020, doi:10.1007/s00520-018-4143-z.
7. Aguado, E.; Mabileau, G.; Goyenvalle, E.; Chappard, D. Hypodynamia Alters Bone Quality and Trabecular Microarchitecture. *Calcif Tissue Int* **2017**, *100*, 332-340, doi:10.1007/s00223-017-0235-x.
8. Arthur, A.; Gronthos, S. Clinical application of bone marrow mesenchymal stem/stromal cells to repair skeletal tissue. *International journal of molecular sciences* **2020**, *21*, 9759.
9. Zhang, Z.C.; He, Q.F.; Zhu, J.H.; Lin, X.X.; Yang, Y.; Chen, H.C.; Huang, X.Q.; Xu, R.G.; Deng, F.L. Optimizing the combined soft tissue repair and osteogenesis using double surfaces of crosslinked collagen scaffolds. *Journal of Biomedical Materials Research Part B-Applied Biomaterials* **2023**, *111*, 1271-1285, doi:10.1002/jbm.b.35231.
10. Sugiama, V.K.; Jeffrey; Naliani, S.; Pranata, N.; Djuanda, R.; Saputri, R.I. Polymeric Scaffolds Used in Dental Pulp Regeneration by Tissue Engineering Approach. *Polymers* **2023**, *15*, doi:10.3390/polym15051082.
11. Guo, T.; Yuan, X.; Li, X.; Liu, Y.; Zhou, J. Bone regeneration of mouse critical-sized calvarial defects with human mesenchymal stem cell sheets co-expressing BMP2 and VEGF. *J Dent Sci* **2023**, *18*, 135-144, doi:10.1016/j.jds.2022.06.020.
12. Otori-Morita, Y.; Niibe, K.; Limraksasin, P.; Nattasit, P.; Miao, X.C.; Yamada, M.; Mabuchi, Y.; Matsuzaki, Y.; Egusa, H. Novel Mesenchymal Stem Cell Spheroids with Enhanced Stem Cell Characteristics and Bone Regeneration Ability. *STEM CELLS TRANSLATIONAL MEDICINE* **2022**, *11*, 434-449, doi:10.1093/stcltm/szab030.
13. Zha, K.K.; Tian, Y.; Panayi, A.C.; Mi, B.B.; Liu, G.H. Recent Advances in Enhancement Strategies for Osteogenic Differentiation of Mesenchymal Stem Cells in Bone Tissue Engineering. *Frontiers in Cell and Developmental Biology* **2022**, *10*, doi:10.3389/fcell.2022.824812.
14. Costela-Ruiz, V.J.; Melguizo-Rodriguez, L.; Bellotti, C.; Illescas-Montes, R.; Stanco, D.; Arciola, C.R.; Lucarelli, E. Different Sources of Mesenchymal Stem Cells for Tissue Regeneration: A Guide to Identifying the Most Favorable One in Orthopedics and Dentistry Applications. *INTERNATIONAL JOURNAL OF MOLECULAR SCIENCES* **2022**, *23*, doi:10.3390/ijms23116356.
15. Chen, X.; Gao, C.Y.; Chu, X.Y.; Zheng, C.Y.; Luan, Y.Y.; He, X.; Yang, K.; Zhang, D.L. VEGF-Loaded Heparinized Gelatine-Hydroxyapatite-Tricalcium Phosphate Scaffold Accelerates Bone Regeneration via Enhancing Osteogenesis-Angiogenesis Coupling. *Frontiers in Bioengineering and Biotechnology* **2022**, *10*, doi:10.3389/fbioe.2022.915181.
16. Camacho-Alonso, F.; Tudela-Mulero, M.R.; Navarro, J.A.; Buendia, A.J.; Mercado-Diaz, A.M. Use of buccal fat pad-derived stem cells cultured on bioceramics for repair of critical-sized mandibular defects in healthy and osteoporotic rats. *Clinical Oral Investigations* **2022**, *26*, 5389-5408, doi:10.1007/s00784-022-04506-w.
17. Su, X.; Wang, T.; Guo, S. Applications of 3D printed bone tissue engineering scaffolds in the stem cell field. *Regen Ther* **2021**, *16*, 63-72, doi:10.1016/j.reth.2021.01.007.
18. Hollinger, J.O.; Kleinschmidt, J.C. The critical size defect as an experimental model to test bone repair materials. *J Craniofac Surg* **1990**, *1*, 60-68, doi:10.1097/00001665-199001000-00011.
19. Furuhashi, M.; Takayama, T.; Yamamoto, T.; Ozawa, Y.; Senoo, M.; Ozaki, M.; Yamano, S.; Sato, S. Real-time assessment of guided bone regeneration in critical size mandibular bone defects in rats using collagen

- membranes with adjunct fibroblast growth factor-2. *J Dent Sci* **2021**, *16*, 1170-1181, doi:10.1016/j.jds.2021.03.008.
20. Peña, G.; Gallego, L.; Redondo, L.M.; Junquera, L.; Doval, J.F.; Meana, Á. Comparative analysis of plasma-derived albumin scaffold, alveolar osteoblasts and synthetic membrane in critical mandibular bone defects: An experimental study on rats. *J Biomater Appl* **2021**, *36*, 481-491, doi:10.1177/0885328221999824.
 21. Xu, L.J.; Yuan, H.; Ye, Q.; Li, J.Y. [Repair of mandibular defects with hydrogel loaded with nano-hydroxyapatite in rats]. *Shanghai Kou Qiang Yi Xue* **2022**, *31*, 449-453.
 22. Bexell, D.; Gunnarsson, S.; Tormin, A.; Darabi, A.; Gisselsson, D.; Roybon, L.; Scheduling, S.; Bengzon, J. Bone Marrow Multipotent Mesenchymal Stroma Cells Act as Pericyte-like Migratory Vehicles in Experimental Gliomas. *Molecular Therapy* **2009**, *17*, 183-190, doi:10.1038/mt.2008.229.
 23. Barzilay, R.; Sadan, O.; Melamed, E.; Offen, D. Comparative characterization of bone marrow-derived mesenchymal stromal cells from four different rat strains. *Cytotherapy* **2009**, *11*, 435-442, doi:10.1080/14653240902849796.
 24. Karaoz, E.; Aksoy, A.; Ayhan, S.; Sariboyaci, A.; Kaymaz, F.; Kasap, M. Characterization of mesenchymal stem cells from rat bone marrow: ultrastructural properties, differentiation potential and immunophenotypic markers. *Histochemistry and Cell Biology* **2009**, *132*, 533-546, doi:10.1007/s00418-009-0629-6.
 25. Harting, M.; Jimenez, F.; Pati, S.; Baumgartner, J.; Cox, C. Immunophenotype characterization of rat mesenchymal stromal cells. *Cytotherapy* **2008**, *10*, 243-253, doi:10.1080/14653240801950000.
 26. Boxall, S.; Jones, E. Markers for Characterization of Bone Marrow Multipotential Stromal Cells. *Stem Cells International* **2012**, *2012*, doi:10.1155/2012/975871.
 27. Song, K.; Huang, M.; Shi, Q.; Du, T.; Cao, Y. Cultivation and identification of rat bone marrow-derived mesenchymal stem cells. *Molecular Medicine Reports* **2014**, *10*, 755-760, doi:10.3892/mmr.2014.2264.
 28. HEMLER, M. VLA PROTEINS IN THE INTEGRIN FAMILY - STRUCTURES, FUNCTIONS, AND THEIR ROLE ON LEUKOCYTES. *Annual Review of Immunology* **1990**, *8*, 365-400, doi:10.1146/annurev.iy.08.040190.002053.
 29. AKIYAMA, S.; HASEGAWA, E.; HASEGAWA, T.; YAMADA, K. THE INTERACTION OF FIBRONECTIN FRAGMENTS WITH FIBROBLASTIC CELLS. *Journal of Biological Chemistry* **1985**, *260*, 3256-3260.
 30. Brown, M.A.; Wallace, C.S.; Anamelechi, C.C.; Clermont, E.; Reichert, W.M.; Truskey, G.A. The use of mild trypsinization conditions in the detachment of endothelial cells to promote subsequent endothelialization on synthetic surfaces. *Biomaterials* **2007**, *28*, 3928-3935, doi:10.1016/j.biomaterials.2007.05.009.
 31. D'Aquino, R.; De Rosa, A.; Laino, G.; Caruso, F.; Guida, L.; Rullo, R.; Checchi, V.; Laino, L.; Tirino, V.; Papaccio, G. Human dental pulp stem cells: from biology to clinical applications. *Journal of Experimental Zoology Part B: Molecular and Developmental Evolution* **2009**, *312B*, 408-415, doi:10.1002/jez.b.21263.
 32. Heitzer, M.; Modabber, A.; Zhang, X.; Winnand, P.; Zhao, Q.; Bläsius, F.M.; Buhl, E.M.; Wolf, M.; Neuss, S.; Hölzle, F.; et al. In vitro comparison of the osteogenic capability of human pulp stem cells on alloplastic, allogeneic, and xenogeneic bone scaffolds.
 33. Merckx, G.; Hosseinkhani, B.; Kuypers, S.; Deville, S.; Irobi, J.; Nelissen, I.; Michiels, L.; Lambrichts, I.; Bronckaers, A. Angiogenic Effects of Human Dental Pulp and Bone Marrow-Derived Mesenchymal Stromal Cells and their Extracellular Vesicles. LID - 10.3390/cells9020312 [doi] LID - 312.
 34. Rombouts, C.; Jeanneau C Fau - Camilleri, J.; Camilleri J Fau - Laurent, P.; Laurent P Fau - About, I.; About, I. Characterization and angiogenic potential of xenogeneic bone grafting materials: Role of periodontal ligament cells.
 35. Luzuriaga, J.; Polo, Y.; Pastor-Alonso, O.; Pardo-Rodríguez, B.; Larrañaga, A.; Unda, F.; Sarasua, J.-R.; Pineda, J.R.; Ibarretxe, G. Advances and perspectives in dental pulp stem cell based neuroregeneration therapies. *International journal of molecular sciences* **2021**, *22*, 3546.
 36. El Moshy, S.; Radwan, I.A.; Rady, D.; Abbass, M.M.; El-Rashidy, A.A.; Sadek, K.M.; Dörfer, C.E.; El-Sayed, K.M.F. Dental stem cell-derived secretome/conditioned medium: the future for regenerative therapeutic applications. *Stem Cells International* **2020**, *2020*.
 37. Sultan, N.; Amin, L.E.; Zaher, A.R.; Scheven, B.A.; Grawish, M.E. Dental pulp stem cells: Novel cell-based and cell-free therapy for peripheral nerve repair. *World Journal of Stomatology* **2019**, *7*, 1-19.
 38. Lan, X.; Sun, Z.; Chu, C.; Boltze, J.; Li, S. Dental pulp stem cells: an attractive alternative for cell therapy in ischemic stroke. *Frontiers in neurology* **2019**, *10*, 824.

39. Man, R.C.; Sulaiman, N.; Idrus, R.B.H.; Ariffin, S.H.Z.; Wahab, R.M.A.; Yazid, M.D. Insights into the effects of the dental stem cell secretome on nerve regeneration: towards cell-free treatment. *Stem cells international* **2019**, *2019*.
40. Bar, J.K.; Lis-Nawara, A.; Grelewski, P.G. Dental Pulp Stem Cell-Derived Secretome and Its Regenerative Potential. *International Journal of Molecular Sciences* **2021**, *22*, 12018, doi:10.3390/ijms222112018.
41. Valluru, M.; Staton Ca Fau - Reed, M.W.R.; Reed Mw Fau - Brown, N.J.; Brown, N.J. Transforming Growth Factor- β and Endoglin Signaling Orchestrate Wound Healing.
42. Patil, A.S.; Sable Rb Fau - Kothari, R.M.; Kothari, R.M. An update on transforming growth factor- β (TGF- β): sources, types, functions and clinical applicability for cartilage/bone healing.
43. Boskey, A.L.; Coleman, R. Aging and Bone. *Journal of Dental Research* **2010**, *89*, 1333-1348, doi:10.1177/0022034510377791.
44. Wu, M.; Chen, G.; Li, Y.P. TGF- β and BMP signaling in osteoblast, skeletal development, and bone formation, homeostasis and disease.
45. Chen, G.; Deng C Fau - Li, Y.-P.; Li, Y.P. TGF- β and BMP signaling in osteoblast differentiation and bone formation.
46. Phillips, A.M. Overview of the fracture healing cascade.
47. Henriksen, K.; Karsdal, M.A.; Martin, T.J. Osteoclast-derived coupling factors in bone remodeling. *Calcif Tissue Int* **2014**, *94*, 88-97, doi:10.1007/s00223-013-9741-7.
48. Huang, J.; Lin, D.; Wei, Z.; Li, Q.; Zheng, J.; Zheng, Q.; Cai, L.; Li, X.; Yuan, Y.; Li, J. Parathyroid Hormone Derivative with Reduced Osteoclastic Activity Promoted Bone Regeneration via Synergistic Bone Remodeling and Angiogenesis. *Small* **2020**, *16*, e1905876, doi:10.1002/smll.201905876.
49. Chen, T.; Wang, Y.; Hao, Z.; Hu, Y.; Li, J. Parathyroid hormone and its related peptides in bone metabolism.
50. Fan, Y.; Hanai, J.-i.; Le, P.T.; Bi, R.; Maridas, D.; DeMambro, V.; Figueroa, C.A.; Kir, S.; Zhou, X.; Mannstadt, M. Parathyroid hormone directs bone marrow mesenchymal cell fate. *Cell metabolism* **2017**, *25*, 661-672.
51. Yang, M.; Arai, A.; Udagawa, N.; Zhao, L.; Nishida, D.; Murakami, K.; Hiraga, T.; Takao-Kawabata, R.; Matsuo, K.; Komori, T. Parathyroid hormone shifts cell fate of a leptin receptor-marked stromal population from adipogenic to osteoblastic lineage. *Journal of Bone and Mineral Research* **2019**, *34*, 1952-1963.
52. Larsson, S.; Jones, H.A.; Göransson, O.; Degerman, E.; Holm, C. Parathyroid hormone induces adipocyte lipolysis via PKA-mediated phosphorylation of hormone-sensitive lipase. *Cellular signalling* **2016**, *28*, 204-213.
53. Jiang, L.; Zhang, W.; Wei, L.; Zhou, Q.; Yang, G.; Qian, N.; Tang, Y.; Gao, Y.; Jiang, X. Early effects of parathyroid hormone on vascularized bone regeneration and implant osseointegration in aged rats. *Biomaterials* **2018**, *179*, 15-28.
54. Keller, J.; Catala-Lehnen, P.; Huebner, A.K.; Jeschke, A.; Heckt, T.; Lueth, A.; Krause, M.; Koehne, T.; Albers, J.; Schulze, J.; et al. Calcitonin controls bone formation by inhibiting the release of sphingosine 1-phosphate from osteoclasts.
55. Yuan, G.; Lu, H.; Yin, Z.; Dai, S.; Jia, R.; Xu, J.; Song, X.; Li, L. Effects of mixed subchronic lead acetate and cadmium chloride on bone metabolism in rats. *Int J Clin Exp Med* **2014**, *7*, 1378-1385.
56. Jeanneau, C.; Le Fournis, C.; About, I. Xenogeneic bone filling materials modulate mesenchymal stem cell recruitment: role of the Complement C5a.
57. Figueiredo, A.; Coimbra P Fau - Cabrita, A.; Cabrita A Fau - Guerra, F.; Guerra F Fau - Figueiredo, M.; Figueiredo, M. Comparison of a xenogeneic and an alloplastic material used in dental implants in terms of physico-chemical characteristics and in vivo inflammatory response.

Disclaimer/Publisher's Note: The statements, opinions and data contained in all publications are solely those of the individual author(s) and contributor(s) and not of MDPI and/or the editor(s). MDPI and/or the editor(s) disclaim responsibility for any injury to people or property resulting from any ideas, methods, instructions or products referred to in the content.